Asian Journal of Chemistry; Vol. 34, No. 6 (2022), 1565-1569

ASIAN JOURNAL OF CHEMISTRY

https://doi.org/10.14233/ajchem.2022.23762

Structural, Optical, Antibacterial and Anticancer Properties of ZnO-TiO_2-GO-Chitosan Nanocomposites Prepared by Coprecipitation Method

V. Sri Priyanka, M.K. Murali* and M. Abdur Rahman

PG and Research Department of Physics, J.J. College of Arts and Science (Autonomous) (Affiliated to Bharathidasan University, Tiruchirappalli), Sivapuram, Pudukkottai-622422 India

*Corresponding author: E-mail: muralimk1970@gmail.com

Received: 4 February 2022; *Accepted*: 29 March 2022; *Published online*: 18 May 2022; AJC-20823

The zinc oxide-titanium dioxide-graphene oxide-chitosan (ZTGCO) nanocomposites were synthesized *via* the chemical precipitation method. The synthesized nanocomposites were characterized by XRD, FTIR, DRS, FESEM, EDAX and PL. The XRD patterns of ZTGCO nanocomposites showed Wurtzite hexagonal structure. The FT-IR spectra represent the various stretching vibrational bands of ZnO, TiO_2, GO and chitosan. The FESEM images revealed that the ZTGCO nanocomposites were in the cauliflower structure. The EDS spectrum showed elemental compositions of ZTGCO with oxygen vacancies. The antibacterial potential of the ZTGCO nanocomposites achieved against *S. aureus* and *E. coli* results showed the ZTGCO had more antibacterial activity than the standard antibiotic amoxicillin. The anticancer activity of the ZTGCO nanocomposites was studied in human liver cancer cells (A549) and the IC_{50} concentration value was observed at 48.67 µg/mL.

Keywords: Chitosan, Biocidal activity, Graphene oxide, Nanocomposites, Coprecipitation.

INTRODUCTION

Microbial infectious diseases often occur due to the contamination of surfaces by many pathogens and constitute a growing threat to public health, causing severe infection problems in the food supply chain, drinking water, household hygiene and the biomedical field [1]. This emerging problem, a biocidal material depends on long-lasting effect, non-toxic and low-cost [2]. Therefore, an antibacterial agent that can prevent bacterial infection has become an active field of research, particularly for biomedical applications. The nanostructure materials are offered higher possibilities to explore biocidal nanomaterials are, increasing, to be employed to other sources of conventional antibiotics the treatment of biocidal properties [3].

In recent decades, ZnO and TiO_2 nanomaterials create considerable attention because of their unique physical, chemical and medical properties [4-6]. The ZnO and TiO_2 nanostructure have potentially enhanced the separation efficiency of photo-excited charge carriers because of the formation of hetero-junction structure between them. The ZnO/TiO_2 nanostructures coupling effects significantly increased the photocatalytic and biocidal activity compared with ZnO and TiO_2 nanomaterials [7,8]. In addition, the modification of metal oxide with graphene oxide and their application in the field of biocidal. Many researchers have mentioned the effect of adding GO to ZnO or TiO_2 nanostructure in terms of oxygen vacancies. Oxygen vacancies in the GO surface matrix of ZnO nanostructures can be enhanced due to the synergetic integration of unique morphology and oxygen vacancies [9]. The GO-TiO_2 thin film highly controlled the *E. coli* bacterial growth compared to TiO_2 film. This maybe due to the presence of graphene oxide increased the inhibition of bacterial growth [10]. However, the combina-torial inorganic-organic materials would be a new opening for clinical-based research due to their unique functionalities. The metal oxide is a potential inorganic biocidal agent if incorporated with biopolymers with antibacterial potentials. Without a doubt, the resulting nanomaterial would have enhanced biocidal capa-city due to the synergistic effect of the two individual materials.

In present investigation, the ZnO-TiO_2-GO-chitosan nano-composites were successfully employed *via* chemical precipi-

tation process. The resulting nanocomposites were characterized for their structural, optical, antibacterial and anticancer properties. Mainly, chitosan was used to improve the bacterial and cell viability of the biocidal properties of the ZnO-TiO_2-GO nanomaterials.

EXPERIMENTAL

Synthesis of ZnO-TiO_2-graphene oxide-chitosan nanocomposite: The ZnO-TiO_2-GO-chitosan nanocomposites were prepared by the chemical method. $Zn(NO_3)_2{\cdot}6H_2O$ (0.1 M) was added with 500 mg of TiO_2 nanoparticles and to 500 mg of GO nanoparticles with addition of 500 mg of chitosan solution and NaOH solution was used as a precipitating agent, 0.1 M of NaOH solution was added into the Zn-TiO_2-GO-chitosan solution, where the black precipitate was obtained. The precipitate was heating 60 ºC with 5 h under magnetic stirrer. The precipitate was cooled at room temperature and washed several times with double distilled water and ethanol. The resulted solution was centrifuged for 15000 rpm with 40 min at -3 ºC. The precipitate was dried at 200 ºC with 2 h.

Antibacterial assay: To determine the antibacterial activity tested against Gram-positive *S. aureus* and Gram-negative *E. coli* bacteria were measured by well diffusion method [5]. The Mueller-Hinton Agar (MHA) medium was transferred into the sterilized petri dishes. A fresh bacteria culture (100 mL) containing 1×10^8 CFU/mL was strike onto the MHA plates by using the sterile swab. The size well of 8 mm diameter was prepared on dishes and the 40 µL:1 mg, 50 µL:1.5 mg and 60 µL:2 mg concentrate solution of ZTGCO nanocomposites dispersed in a 5% of sterilized DMSO were filled inside well and petri plate were incubation 24 h at 37 ºC and there after zone of inhibition was measured. The reference antibiotic was used as amoxicillin (30 µg). Antibacterial potential assay was carried out triplicate [11,12].

MIC and MBC determination: The minimum amount of concentration, ZTGCO nanocomposites is required to inhibit the bacterial activity was measured by supplement the various concentration (0.1-2.0 mg/mL) of nanocomposites into the bacterial cultures and 24 h of incubation. Bacterial culture was plated and the growth culture was measured through the colony formation method. The minimum concentration and there was no visual growth on culture plates. The minimum bactericidal concentration (MBC) was the last dilution in which no bacterial regrowth on bacterial culture plates [13,14].

SEM analysis of bacteria: Untreated (alone) and ZTGCO nanocomposites treated with a minimum inhibitory concentration of *S. aureus* cells were centrifuged at 4000 rpm for 20 min at 4 ºC; the untreated *S. aureus* cells remained as the control. The bacterial cells pellet collected were gently washed, with distilled water and fixed with 2.5% glutaraldehyde in double distilled water at 4 ºC for 2 h. Whereas after fixation, the bacterial sample was washed with double distilled water and dehydrated with a series of various percentages of (25%, 50%, 75% and 100%) ethanol concentrations. The dehydrated control and the ZTGCO nanocomposites treated *S. aureus* sample was kept for 12 h in a desiccator and gold-coated by the sputtering method. The prepared *E. coli* bacterial sample was analyzed by SEM.

MTT assay: Cell viability test, liver cancer (A549) viable cells were harvested and counted using haemocytometers diluted in Dulbecco's modified eagle medium (DMEM) medium to a density of 1×10^4 cells/mL was seeded in 96 well plates for each well and incubated for 24 h to allow attachment. After A549 cells were treated with control and containing various concentrations of ZTGCO nanocomposites 10 to 100 µg/mL were applied to each well. A549 cells were incubated at 37 ºC in a humidified 95% air and 5% CO_2 incubator for 24 h. After incubation, the ZTGCO nanocomposites containing cells wash with fresh culture medium and the MTT (5 mg/mL in PBS) dye was added to each well plate, followed by incubated for another 4 h at 37 ºC. The purple precipitated formazan formed was dissolved in 100 µL of concentrated DMSO and the cell viability was absorbance and measured 540 nm using a multi-well plate reader.

Characterization: The ZTGCO nanocomposites was characterized by X-ray diffractometer (model: X'PERT PRO PANalytical). The diffraction patterns were recorded in the range of 20-80º for the ZTGCO sample where the monochromatic wavelength of 1.54 Å was used. NanoPlus dynamic light scattering (DLS) nanoparticle sizer was used for the particle size analysis of the ZTGCO nanocomposites. The spectrum of the FTIR was recorded in the wavenumber range of between 4000-400 cm^{-1} by using Perkin-Elmer spectrometer. The Photoluminescence (PL) spectra were taken by using the spectrometer, Perkin Elmer-LS 14.

RESULTS AND DISCUSSION

XRD studies: The XRD patterns of ZnO-TiO_2-GO-chitosan nanocomposites are shown in Fig. 1. The lattice planes of ZTGCO nanocomposites (1 0 0), (0 0 2), (1 0 1), (1 0 2), (1 1 0), (1 0 3), (2 0 0), (1 1 2), (2 0 1), (0 0 4) and (2 0 2) with difference angles at (2θ) 31.70º, 34.39º, 36.19º, 47.50º, 56.51º, 62.80º, 66.34º, 67.88º, 68.98º for ZnO phase formation, these *hkl* planes are perfectly matched with the hexagonal structure (JCPDS no. 36-1451). To observed some additional diffraction peaks at (9.41º and 43.21º) and (25.72º, 29.82º and 48.51º) corresponding to the GO and TiO_2 incorporation. Moreover, the chitosan is typically non-crystalline biopolymer peaks observed at 10.88º and 20.60º. This formation indicates that the combination of ZnO, TiO_2, GO and chitosan phases formation is due to both the steric effects and the intermolecular hydrogen bonds between the ZnO-TiO_2-GO-chitosan surface matrix. The average crystallite size of ZnO-TiO_2-GO-chitosan nanocomposites calculated by the Debye-Scherrer's formula was 62 nm.

FT-IR studies: The FT-IR spectrum of ZnO-TiO_2-GO-chitosan nanocomposites is shown in Fig. 2, which revealed that the ZnO, TiO_2, GO and chitosan functional groups were observed in the ZTGCO sample. The O-H and N-H stretching vibration were observed at 3416 cm^{-1}, symmetric and asymmetric C-H stretching located at 2930 and 2852 cm^{-1}, C=C and C-OH stretching were observed at 1631 and 1151 cm^{-1}, which correspond to carbonyl, the carboxyl groups are responsible

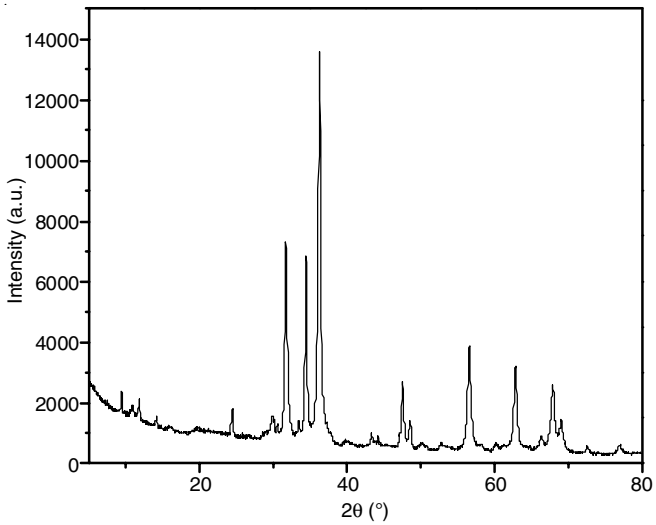

Fig. 1. X-ray diffraction patterns of ZTGCO nanocomposites

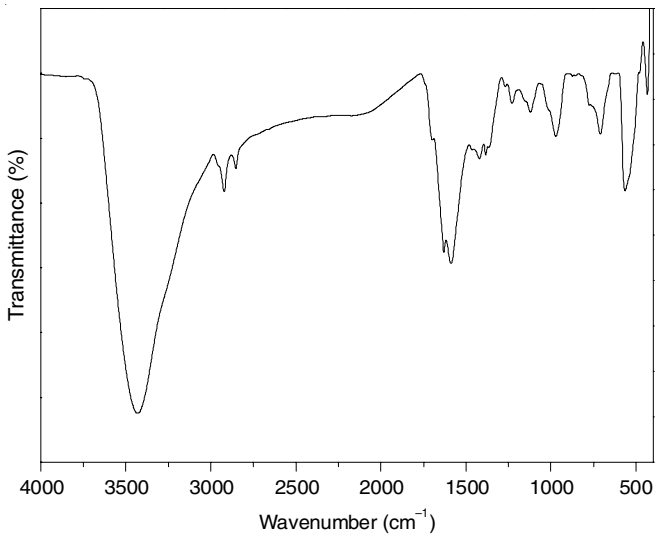

Fig. 2. FT-IR spectrum of ZnO-TiO_2-GO-chitosan nanocomposites

for the origin of oxygen species on GO. Furthermore, the metal-oxygen stretching vibration like Zn-Ti-O was identified at 777, 711, 620 and 434 cm^{-1}. This FTIR spectrum of ZnO-TiO_2-GO-chitosan nanocomposites exhibited the metal-oxygen, carboxyl group and hydroxyl groups and amine groups were present in the sample synergetic effect between GO, TiO_2 and ZnO. This result might implies that the chitosan, ZnO and TiO_2 nanostructure were firmed attached to the GO surface sheets. The FT-IR spectrum confirmed that ZnO-TiO_2-GO-chitosan nanocomposites could some oxygen-containing functional groups and defect sites. As a result, it revealed a strong interaction between chitosan, GO, TiO_2 and ZnO nanocomposites.

Particle size analysis: Dynamic light scattering (DLS) study provide the information about size distribution the particle size in suspension, using an aqueous solution. The sizes (nanoparticle itself, surrounded by water molecules) of the ZnO-TiO_2-GO-chtiosan nanocomposites were observed at ~130.70 nm (Fig. 3). However, the DLS particle size increased when compared to the XRD results, since ZnO-TiO_2-GO-chitosan was surrounded by water molecules and known as hydrodynamic size.

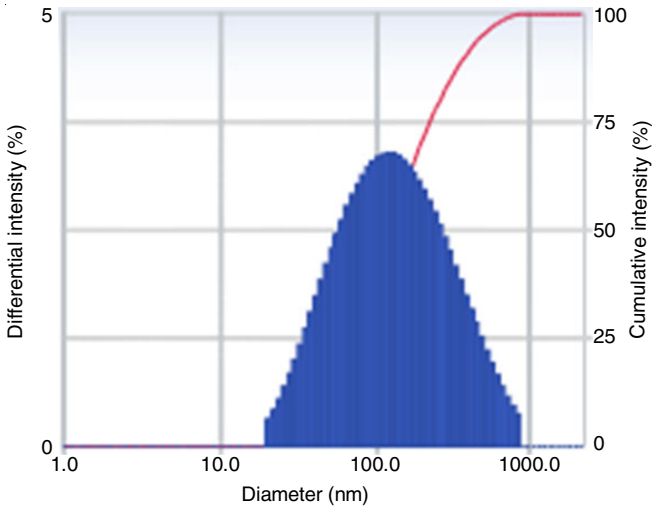

Fig. 3. DLS spectrum of ZnO-TiO_2-GO-chitosan nanocomposites

Morphology studies: The morphology of ZnO-TiO_2-GO-chitosan nanocomposites was analyzed *via* a FESEM technique. The ZTGCO nanocomposites exhibited GO surface is decorated with ZnO-TiO_2-chitosan cauliflower structure with uniform distribution nanomaterials (Fig. 4). These results demonstrated the ZnO-TiO_2-chitosan nanostructure increased more free surface area or grain boundaries and improved the surface interaction due to the GO sheet addition. The increased surface area of ZnO-TiO_2-GO-chitosan nanocomposites can be suitable for biocidal activity such as antibacterial and anticancer properties.

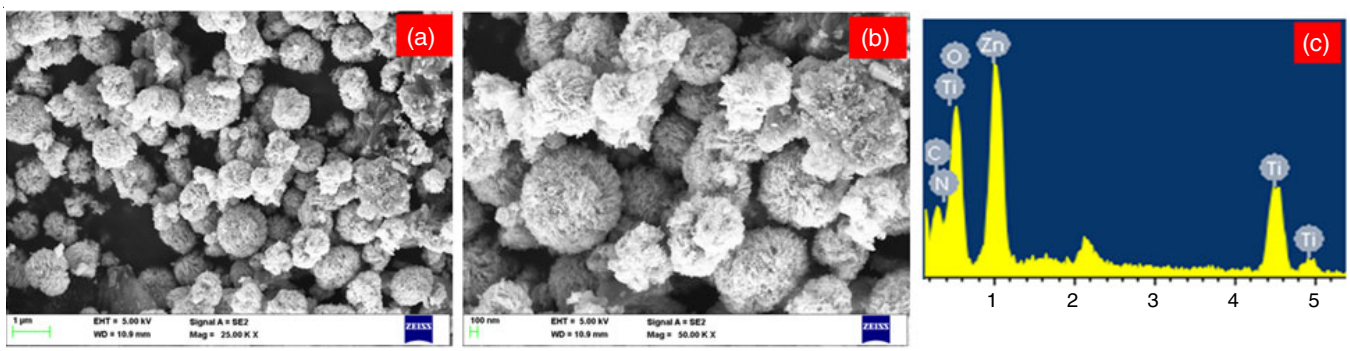

Fig. 4. (a-b) Lower and higher magnification FESEM image and (c) EDX spectrum of ZnO-TiO_2-GO-chitosan nanocomposites

The chemical composition of ZTGCO nanocomposites was identified by a typical EDX spectrum (Fig. 4c). The atomic percentages were found to be 23.61 % (C), 7.35% (N) 25.49% (Zn), 18.68% (Ti) and 24.87% (O) for ZnO-TiO_2-GO-chitosan nanocomposites.

Photoluminescence (PL) studies: The photoluminescence emission spectrum of ZnO-TiO_2-GO-chitosan nanocomposites have two peak positions in the UV-visible regions and excitation wavelength of 325 nm is shown in Fig. 5. The emission spectrum of ZnO-TiO_2-GO-chitosan nanocomposites exhibited six peaks at 384, 422, 443, 457, 478 and 517 nm, respectively. The UV peaks at 384 nm were for near-edged emissions, whereas the peak at 422 nm denotes the violet emission for natural zinc interstitials (Zn_i). The peaks at (443, 457 and 478 nm) represent the blue emission due to zinc vacancy (V_{zn}) and oxygen vacancy (O_V), respectively. The peak at 517 nm denotes green emission for oxygen vacancies (O_V).

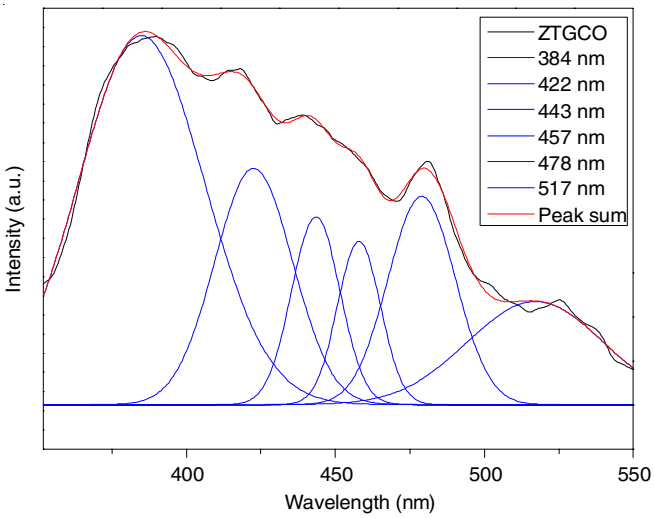

Fig. 5. PL spectrum of ZnO-TiO_2-GO-chitosan nanocomposites

Antibacterial activity: The antibacterial activity of ZnO-TiO_2-GO-chitosan nanocomposites showed similar activity as the zone of inhibition (ZOI) for amoxicillin, with tested against *S. aureus* and *E. coli* bacterial strains tested different concentration ranges of 1-2 mg/mL and resulted in the ZOI in the range of 10-18 mm as shown in Fig. 6. The MIC and MBC values of ZnO-TiO_2-GO-chitosan nanocomposites against *S. aureus* and *E. coli* were 0.9 and (1.2 and 1.5 mg/mL), respectively (Table-1). Thus, the membrane damage of bacteria may be caused by electrostatic interaction between composites and cell surfaces, cellular internalization and the generation of reactive oxygen species including H_2O_2 in cells due to ZnO-TiO_2-GO-chitosan nanocomposites.

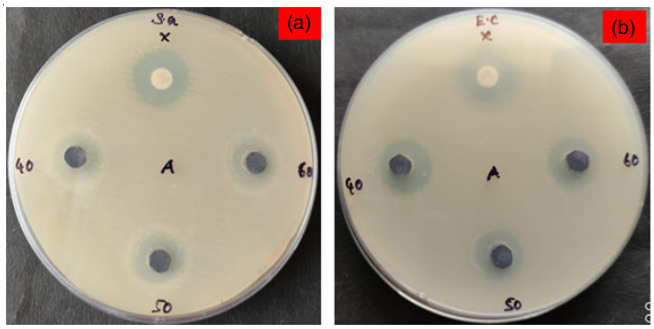

Fig. 6. Antibacterial activity of ZnO-TiO_2-GO-chitosan nanocomposites

TABLE-1
MEASUREMENT OF MIC AND MBC VALUES FOR ZTGCO NANOCOMPOSITES TREATED WITH *S. aureus* AND *E. coli*

Concentration of ZTGCO (mg/mL)	Effect of ZTGCO nanocomposites on the G (+) and G (-) bacterial strains	
	S. aureus	*E. coli*
0.1	Live	Live
0.3	Live	Live
0.6	Live	Live
0.9	Bacteriostatic (MIC)	Bacteriostatic (MIC)
1.2	Bacteriostatic	Bactericidal (MBC)
1.5	Bactericidal (MBC)	Bactericidal
1.8	Bactericidal	Bactericidal
2.0	Bactericidal	Bactericidal

The morphological changes were observed in *S. aureus* bacterial cells culture treated with ZTGCO nanocomposites were confirmed through SEM analysis to view for structural integrity and cell damage (Fig. 7). The untreated group (control cells) does not display any injury to the cell membrane (Fig.

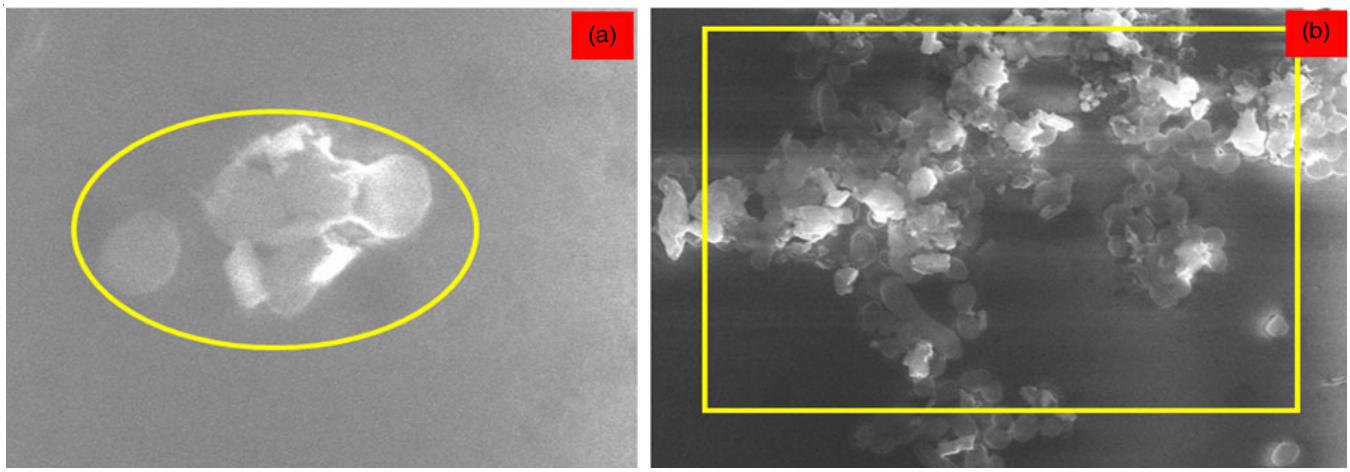

Fig. 7. (a-b) Morphological studies of *S. aureus* treated with ZnO-TiO_2-GO-chitosan nanocomposites

7a). The ZTGCO nanocomposites were treated with *S. aureus* group; the cells are denoted by the square (Fig. 7b). For ZTGCO, nanocomposites were to stick to the surface of the bacterial outer cell membrane. The interaction of nanocomposites leads to the disruption and disorganization of the membranes [3]. As a result, the microbes were loss in cell viability.

Anticancer activity: *In vitro* anticancer activity was performed against human liver cancer cells (A549) with different concentrations (10-100 µg/mL) of synthesized ZTGCO nanocomposites *via* an MTT assay. After 24 h of exposure, the optimized amount of ZTGCO composites penetrated the cells, confirmed by IC_{50} cell viability in 48.67 µg/mL (Fig. 8). The cytotoxicity of ZTGCO nanocomposites depends on various parameters such as particle size, increasing surface-volume ratio, surface defects (oxygen vacancies) and the morphology (uneven ridges) of the particles [15,16]. In present work, the ZTGCO nanocomposite has more surface defects (oxygen vacancies) and uneven surface ridges (cauliflower structure) formation in ZTGCO nanocomposites. These results in solid anticancer activity against liver cancer cells.

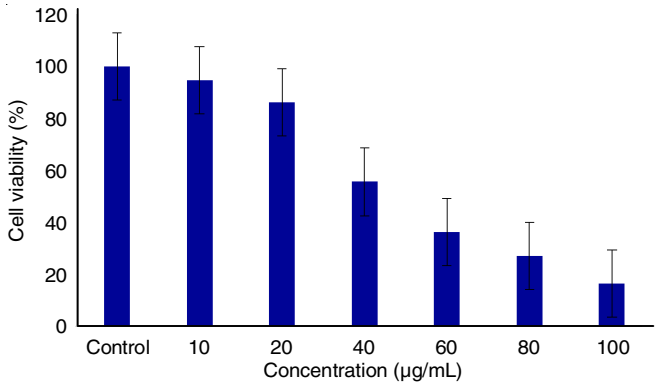

Fig. 8. A549 cells were tested on different concentrations of (10-100 µg/mL) for ZTGCO nanocomposites at 24 h

Conclusion

In summary, zinc oxide-titanium dioxide-graphene oxide-chitosan (ZTGCO) nanocomposites were prepared by the chemical precipitation method. The X-ray diffraction study confirmed that the prepared ZnO-TiO_2-GO-chitosan composites were of the hexagonal structure. From the DLS studies, the ZnO-TiO_2-GO-chitosan nanocomposites sizes were observed at ~130.70 nm. The ZTGCO nanocomposites exhibited GO surface was decorated with ZnO-TiO_2-GO-chitosan cauliflower structure with uniform distribution composites. The metal-oxygen stretching vibration like Zn-Ti-O was identified. The photoluminescence spectra of ZnO-TiO_2-GO-chitosan revealed oxygen vacancies at 517 nm, respectively. The antibacterial test performed against *S. aureus* and *E. coli* confirmed that the ZTGCO nanocomposites had a higher antibacterial potential as compared to conventional antibiotic amoxicillin. The cytotoxicity studies were also performed against human liver cancer lines using prepared ZTGCO nanocomposites.

CONFLICT OF INTEREST

The authors declare that there is no conflict of interests regarding the publication of this article.

REFERENCES

1. M. Abdallah, C. Benoliel, D. Drider, P. Dhulster and N.E. Chihib, *Arch. Microbiol.*, **196**, 453 (2014); https://doi.org/10.1007/s00203-014-0983-1
2. A. Munoz-Bonilla and M. Fernandez-Garcia, *Eur. Polym. J.*, **65**, 46 (2015); https://doi.org/10.1016/j.eurpolymj.2015.01.030
3. C. Karthikeyan, K. Varaprasad, A. Akbari-Fakhrabadi, A.S.H. Hameed and R. Sadiku, *Carbohydr. Polym.*, **249**, 116825 (2020); https://doi.org/10.1016/j.carbpol.2020.116825
4. P. Bansal, G. Singh and H.S. Sidhu, *Mater. Chem. Phys.*, **257**, 123738 (2021); https://doi.org/10.1016/j.matchemphys.2020.123738
5. S.O. Aisida, A. Batool, F.M. Khan, L. Rahman, A. Mahmood, I. Ahmad, T. Zhao, M. Maaza and F.I. Ezema, *Mater. Chem. Phys.*, **255**, 123603 (2020); https://doi.org/10.1016/j.matchemphys.2020.123603
6. A. Ulu, E. Birhanli, S. Köytepe and B. Ates, *Int. J. Biol. Macromol.*, **163**, 529 (2020); https://doi.org/10.1016/j.ijbiomac.2020.07.015
7. M. Guo, W. Jiang, C. Chen, S. Qu, J. Lu, W. Yi and J. Ding, *Energy Convers. Manage.*, **229**, 113745 (2021); https://doi.org/10.1016/j.enconman.2020.113745
8. Y. Rilda, D. Damara, Y.E. Putri, R. Refinel, A. Agustien and H. Pardi, *Heliyon*, **6**, e03710 (2020); https://doi.org/10.1016/j.heliyon.2020.e03710
9. M.K. Kavitha, P. Gopinath and H. John, *Phys. Chem. Chem. Phys.*, **17**, 14647 (2015); https://doi.org/10.1039/C5CP01318F
10. A. Jalaukan, S.A.M. Aldowaib, A.S. Hammed, B.G. Shohany, R. Etefagh and A.K. Zak, *Iran. J. Mater. Sci. Eng.*, **16**, 53 (2019); https://doi.org/10.22068/ijmse.16.4.53
11. S. Harinee, K. Muthukumar, A. Abirami, K. Amrutha, K. Dhivyaprasath and M. Ashok, *Adv. Mater. Process.*, **4**, 115 (2021); https://doi.org/10.5185/amp.2019.0006
12. M. Krishnan, H. Subramanian, H.-U. Dahms, V. Sivanandham, P. Seeni, S. Gopalan, A. Mahalingam and A.R. Rathinam, *Sci. Rep.*, **8**, 2609 (2018); https://doi.org/10.1038/s41598-018-20718-1
13. M. Krishnan, V. Sivanandham, D. Hans-Uwe, S.G. Murugaiah, P. Seeni, S. Gopalan and A.J. Rathinam, *Mar. Pollut. Bull.*, **101**, 816 (2015); https://doi.org/10.1016/j.marpolbul.2015.08.033
14. S. Harinee, K. Muthukumar, H.-U. Dahms, M. Koperuncholan, S. Vignesh, R.J. Banu, M. Ashok and R.A. James, *Int. Biodeterior. Biodegrad.*, **145**, 104790 (2019); https://doi.org/10.1016/j.ibiod.2019.104790
15. M. Krishnan, H.-U. Dahms, P. Seeni, S. Gopalan, V. Sivanandham, K. Jin-Hyoung and R.A. James, *Mater. Sci. Eng. C*, **73**, 743 (2017); https://doi.org/10.1016/j.msec.2016.12.062
16. I. Matai, A. Sachdev, P. Dubey, S. Uday Kumar, B. Bhushan and P. Gopinath, *Colloids Surf. B Biointerfaces*, **115**, 359 (2014); https://doi.org/10.1016/j.colsurfb.2013.12.005